Influence of a sedimentary basin infilling description on the 2D P-SV wave propagation using linear and nonlinear constitutive models

C. Gélis
IRSN, France

L.F. Bonilla
Université Paris Est - IFSTTAR, France

SUMMARY:
Numerical modeling is a useful tool to understand the role of different parameters (site geometry, impedance contrast, material properties, constitutive model, input solicitation) governing site effects. We focus here on the 2D P-SV seismic wave propagation in a simple-shaped asymmetric model. We consider two ways of describing the sedimentary infilling properties: the basin is either composed of distinct homogeneous geological layers or is described through properties progressively changing as a function of depth (gradient-based model). We assess the influence of these two assumptions on the wave propagation while taking into account linear and nonlinear constitutive models. We show that the shear strain highest values are located in a layered basin at superficial layers bottoms where high impedance contrasts lead to wave amplification. The presence of nonlinearity generally enhances wave amplification at the layers bottoms. In a gradient-based model, the shear strain highest values are also controlled by nonlinear properties discontinuities.

Keywords: Site response, 2D P-SV, nonlinear, viscoelastic, basin description

INTRODUCTION

Basin response depends on the site geometry, impedance contrast, material properties and their constitutive model, and on the complexity and strength of the input solicitation. Numerical modeling is a useful tool to understand the role and the influence of these different parameters governing site effects. To compute the basin response, one has first to build a geological/geotechnical model based on available data, such as the geological knowledge, invasive borehole or cross-hole measurements, non-destructive seismic measurements like surface wave analysis and ambient noise. Depending on the available data and on the assumptions used, one may build a model with homogeneous layers or a model whose properties progressively change as a function of depth. As an example, Lacave and Lemeille (2006) propose three models for the internal structure of the alpine valleys; among them, the first two are composed of homogeneous layers whereas in the last one, P and S velocities smoothly increase with depth.

From a modeling point of view, assumptions made while building a velocity model may strongly affect the basin response. In order to assess the influence of the basin sedimentary infilling assumption on the wave propagation, we study in this paper the response of an asymmetrical simple-shape basin which is either composed of distinct homogeneous geological layers or is described through properties progressively changing as a function of depth (gradient-based model). In order to study the wave propagation in two basins with similar soil properties, P and S velocities of the layered basin are deduced from the gradient-based basin ones while density, intrinsic attenuation and nonlinear properties remain equal in both models.

We first explain in the following the numerical method used to model 2D P-SV in linear and nonlinear soils. We then present the numerical models used in this study: waves emitted by two different input motions are propagated in the two basins in linear and nonlinear media. We assess the influence of the basin sedimentary infilling assumption on the wave propagation through the spatial distribution of the maximum shear strain in each basin model.

1. NUMERICAL MODELLING OF 2D P-SV WAVE PORPAGATION USING LINEAR AND NONLINEAR CONSTITUTIVE MODELS

1.1. 2D P-SV elastic waves propagation

Wave equation is solved assuming an isotropic medium using the Finite Differences Method following the stencil of Saenger et al. (2000). The free surface is introduced by zeroing the Lamé coefficients, corresponding to the vacuum formulation used by Saenger et al. (2000). Gélis et al. (2005) showed that this formulation of surface condition in the Saenger's stencil allows to precisely modeling the surface waves propagation. Yet, this stencil requires 15 to 30 points per minimum Rayleigh wavelength in presence of free surface without topography (Bohlen and Saenger, 2006).

1.2. Constitutive models

When waves are propagating through a medium, part of the energy is converted to heat and is lost during the propagation. This phenomenon called intrinsic attenuation is thought not to depend on frequency or on shear deformation level. To model the wave propagation in a viscoelastic model, we follow the technique of Liu and Archuleta (2006) based on a generalized Maxwell model (Day and Bradley, 2001). In the technique of Liu and Archuleta (2006), energy is dissipated through the use of memory variables that allow to implementing constant attenuation between 0.1 and 50 Hz through quality factors ranging between 5 and 5000.
In the case of strong motion propagating on soft soils, the shear strain becomes significant and nonlinear soil behavior may take place (Iai et al., 1995; Ishihara, 1996). In this study, we adopted the nonlinear soil rheology proposed by Towhata and Ishihara (1985) and Iai et al. (1990). This is a plane strain model that is relatively easy to implement and needs only the angle of friction and the cohesion when pore pressure is not taken into account, which is the case in this paper. The material strength is computed following a Coulomb's criterion, and the stress-strain relation follows the hyperbolic model. Bonilla et al. (2005) modified the nonlinear constitutive model of Towhata and Ishihara (1985) and Iai et al. (1990) so that hysteresis cycles are assured by applying the Generalized Masing Rules operator.
In order to take into account low strains damping (viscoelastic part) and hysterestic attenuation (nonlinear part), we follow Assimaki et al. (2010) approach where the total energy dissipated in the soil is equal to the sum of attenuation related to small shear strain damping modeled with the technique of Liu and Archuleta (2006) and hysteretic damping accounted for through the nonlinear constitutive model. More details and discussion about the numerical implementation of soil constitutive models in the Saenger et al. (2000) finite difference scheme can be found in Gélis and Bonilla (2012).

2. NUMERICAL MODEL

2.1. Basin geometry and properties

Figure 1 shows the basin asymmetrical shape. This 500-m large and 225-m deep basin is similar to those found in the European Alpine basins (Lacave and Lemeille, 2006). Following their study (third proposed model), the shear wave velocity Vs (in m/s) is considered to gradually increase with depth z (in meters) as:

$$Vs = 200 + 50\sqrt{z} \qquad (2.1)$$

The shear wave velocity therefore ranges from 200 m/s at the basin surface to 950 m/s at the basin bottom and is 2000 m/s in the bedrock outside the basin. Table 1 shows the basin and bedrock properties.
Figure 2 shows the shear modulus reduction and damping ratio curves as a function of the shear deformation defining the nonlinear properties of six different soils that are used in this study. These curves are defined by EPRI (1993) and account for the nonlinear behaviour of sands as a function of depth. Soils located at shallower depth are more nonlinear than soils located at greater depths. The damping is zero at small strains. In this analysis, we use depth limits defined in EPRI (1993) to

determine the soil nonlinear properties at each depth. Table 2 shows depth range validity, γ_{ref} (shear strain at G/Gmax=0.5) and maximum damping for each curve.
These depth ranges define layers where nonlinear properties are constant. We compute for each layer the mean shear wave velocity (table 2). Using these values as well as the soil properties reported in table 1 allows defining the properties of a layered medium, which is shown in figure 3. P and S velocities are therefore different in the gradient-based and the layered basins whereas density and nonlinear properties remain equal in both models. On the contrary, two different assumptions are made regarding the intrinsic attenuation : it depends on the velocities in the gradient-based model whereas it is kept constant in the layered model. The comparison between results obtained with both basin models will allow quantifying the influence of the basin sedimentary infilling assumption on the wave propagation.

Table 1. Basin and bedrock properties

	Basin (gradient model)	Basin (layered model)	Bedrock
Poisson ratio	0.45	0.45	0.35
Qp	0.1*Vp	40	400
Qs	0.1*Vs	20	200
Volumetric mass (kg/m3)	1800	1800	2200

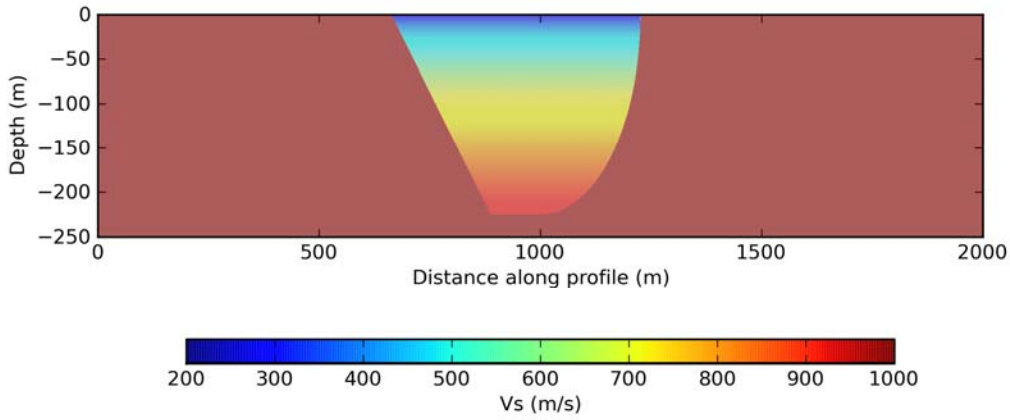

Figure 1. Shear wave velocity gradient-based model. Vs=2000 m/s in the bedrock.

2.2. Input seismic motion and model discretization

Figure 4 shows the two sources used in this study as input motion and acting as vertical incidence plane SV waves. In this figure, the corresponding PGA (Peak Ground Acceleration) of both sources is 0.25g at the bedrock free surface. Although not realistic, we use the simple Gabor-type source because it allows studying the wave propagation over a large frequency band (0.1 – 15 Hz) with an acceleration wavelet having only two loading-unloading cycles. On the contrary, seismic waves emitted by a fault are much more complex. The source duration is higher and the radiated seismic waves contain low frequency information from the rupture process. Figure 4 shows the first 15 seconds of a real seismogram corresponding to the N-S horizontal component of the ground motion recorded on a rock site during the 1994 Northridge earthquake (Hartzell et al., 2004) whose PGA is also scaled to 0.25g at surface. Energy is present in a narrower frequency band (0.1 – 8 Hz). With such a complex source, loading and unloading cycles occur successively and nonlinearity may be activated during a longer time.
For all computations, the time step is 2.5.10 -5 s and the space step is 0.25 m following the Courant-Friedrich-Lewy stability criterion for the Saenger et al. (2000) finite difference stencil. Absorbing boundary conditions (Cerjan et al., 1985) are implemented at the basis of the basin to avoid reflections from the model's bottom; whereas periodic conditions are implemented on the model edges. Looking at the frequency content of both sources, this leads to a minimum S wavelength in the basin of 15 m

for the Gabor-type source and to 25 m for the Northridge source. The chosen spatial discretization fulfils the required number of points per minimum wavelength of Bohlen and Saenger (2006) in the linear case. As we do not know a priori how much we enter in the nonlinear regime, we spatially oversample the model in the linear case and we check a posteriori that the required number of points per minimum wavelength of Bohlen and Saenger (2006) is satisfied with the nonlinear constitutive model. Making this checking after the simulation is important to avoid numerical dispersion.

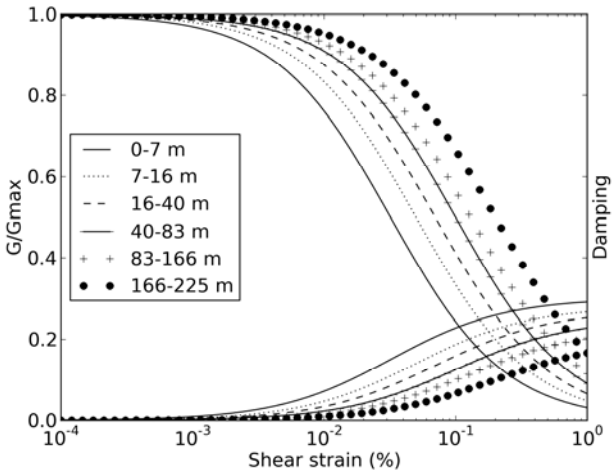

Figure 2 (Shear modulus G, damping ratio D, shear strain γ) curves for cohesionless material located at six different depths (EPRI, 1993). Damping is zero at small shear strains.

Table 2. Nonlinear properties and mean shear wave velocity for each layer.

Depth range	γ_{ref}	Maximum damping	Mean Vs (layered model)
0-7 m	$3.2.10^{-4}$	0.3	278.5 m/s
7-16 m	5.10^{-4}	0.28	362.4 m/s
16-40 m	7.10^{-4}	0.27	456.9 m/s
40-83 m	1.10^{-3}	0.25	585.2 m/s
83-166 m	13.10^{-3}	0.23	749.8 m/s
166-225 m	2.10^{-3}	0.2	897.5 m/s

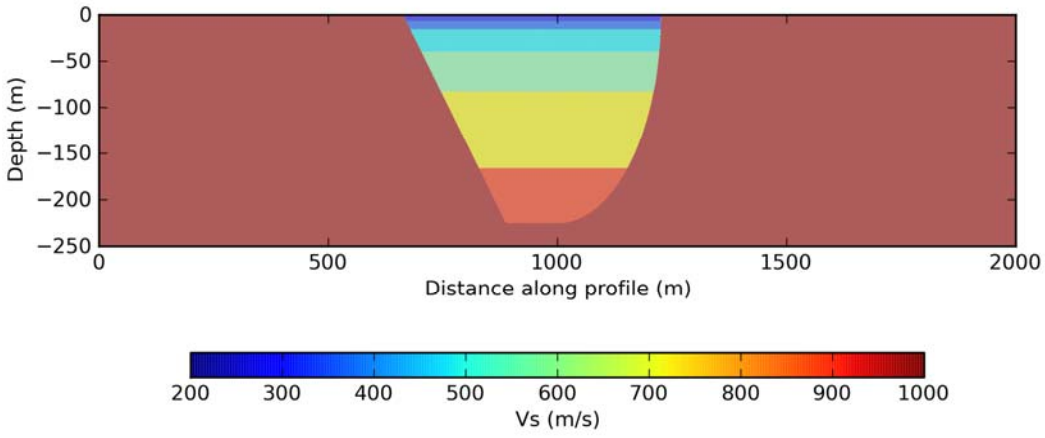

Figure 3. Shear wave velocity layered model. Vs=2000 m/s in the bedrock.

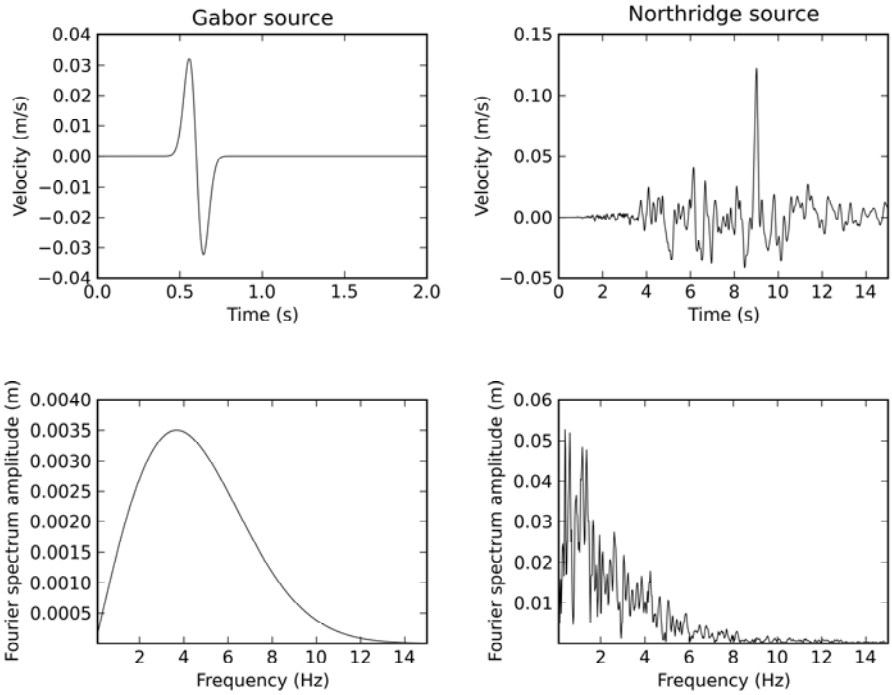

Figure 4. Input seismic motion (velocity field)

3. INFLUENCE OF THE BASIN FILLING

3.1. Viscoelastic soil

Figure 5 shows the standard spectral ratio (SSR) computed in the gradient-based and the layered models in a viscoelastic soil using the Gabor input motion. On the whole, SSR shapes are very similar because basin properties (geometry and properties) are very close together. However, amplification is stronger at high frequencies in the gradient-based model in which the intrinsic attenuation is lower (table 1). This is due to the progressive wave amplification related with velocity decrease while waves are propagated towards the surface. Moreover, velocity at the free surface is lower in the gradient-based basin (Vs=200 m/s) than in the layered model (Vs=278.5 m/s).

Figure 6 shows the maximum shear strain calculated at each grid point during the wave propagation for the gradient-based and the layered models using the Gabor or the Northridge input motions. In general, maximum shear strain is higher in low velocity zones located near the free surface. As shown in Gélis and Bonilla (2012), maximum shear strain is higher with the Northridge input motion due to a higher number of cycles and a longer duration even if both sources have the same PGA. Highest values are reached at a depth that depends on the source spectral content: they are deeper with the Northridge input motion than with the Gabor higher-frequency one. This is clearly visible when the shear wave velocity progressively increases with depth (gradient-based basin). When the basin is layered, the stronger and sharper impedance contrasts between layers lead to the wave amplification at the bottom of each layer. Therefore the maximum shear strain is higher at the layers bottom.

Figure 7 shows the logarithm base 10 of the ratio between the maximum shear strain calculated in the layered basin and the gradient-based model with both sources. This ratio is a function of the input motion because it depends on the dominant wavelength controlled by the input spectral content. Figure 7 clearly shows that shear strain is higher at the layers bottom and lower at the layers top in the layered model than in the gradient-based model whatever the input motion. Just under the free surface, shear strain is higher in the gradient-based model, which is consistent with the higher SSR amplification shown in figure 5.

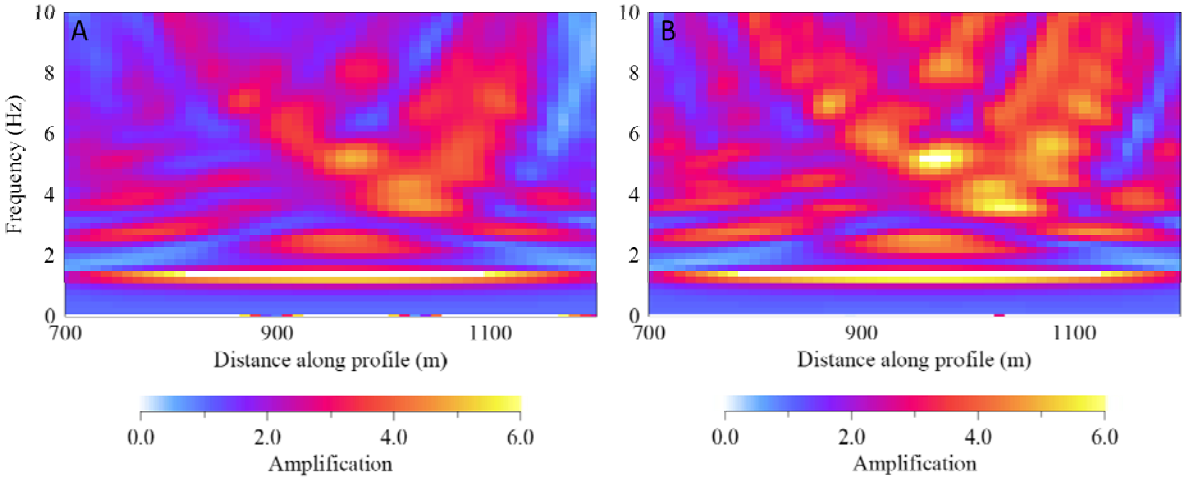

Figure 5. Standard Spectral Ratio for receivers located at the free surface for (A) the layered basin and (B) the gradient-based basin with a viscoelastic soil.

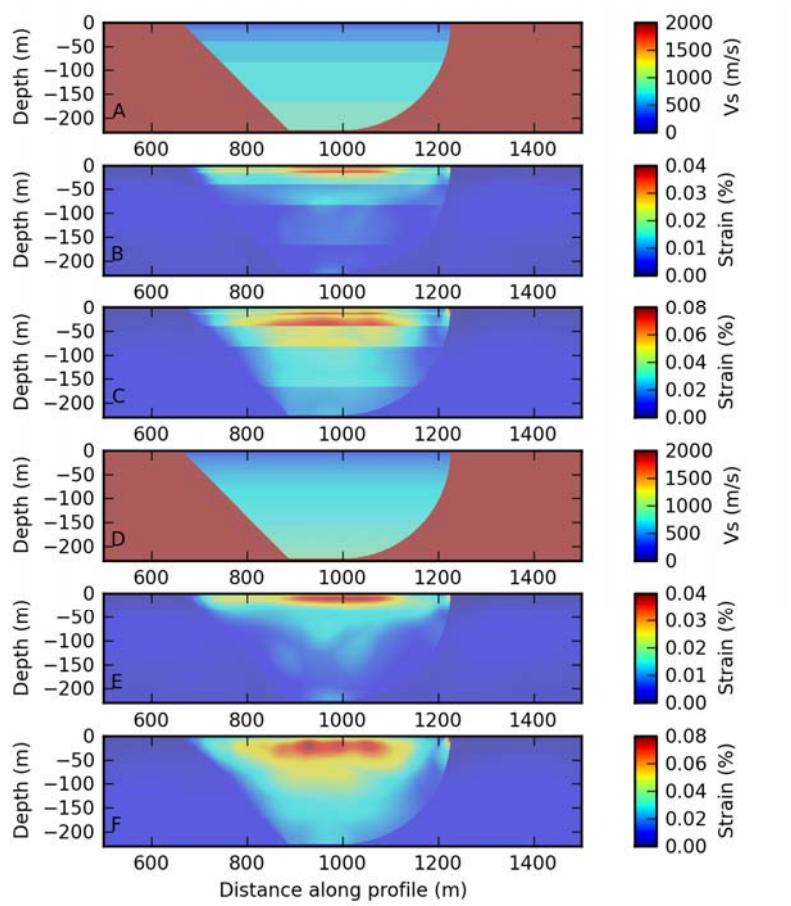

Figure 6. Maximum shear strain calculated in the layered basin (A) and gradient-based basin (D) respectively with the Gabor input motion (B, E) and Northridge input motion (C, F) in a viscoelastic soil.

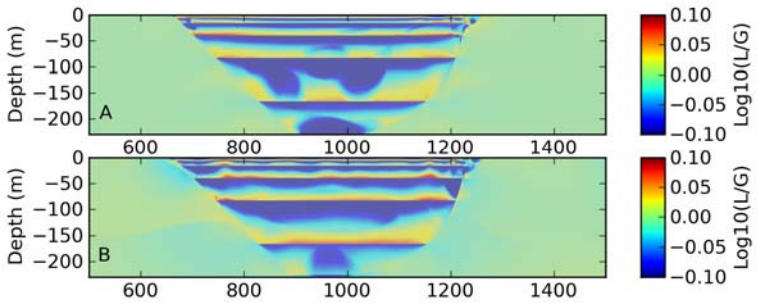

Figure 7. Ratio between the maximum shear strain calculated in the layered basin L and the gradient-based model G with (A) the Gabor input motion and (B) the Northridge one in the viscoelastic soil.

3.2. Visco-elastoplastic soil

Figure 8 shows the standard spectral ratio (SSR) computed in the gradient-based and the layered models in a visco-elastoplastic soil using the Gabor input motion. In comparison with figure 5, high frequencies are damped due to nonlinear effects. SSR shapes are very similar and the amplifications in both basins are very close together with a visco-elastoplastic soil even if amplification is lightly stronger in the gradient-based basin. Therefore nonlinearity tends to reduce differences between SSR computed at the free surface in the two basins. However, as shown in Gélis and Bonilla (2012), effects of nonlinearity on SSR strongly depend on the input motion.

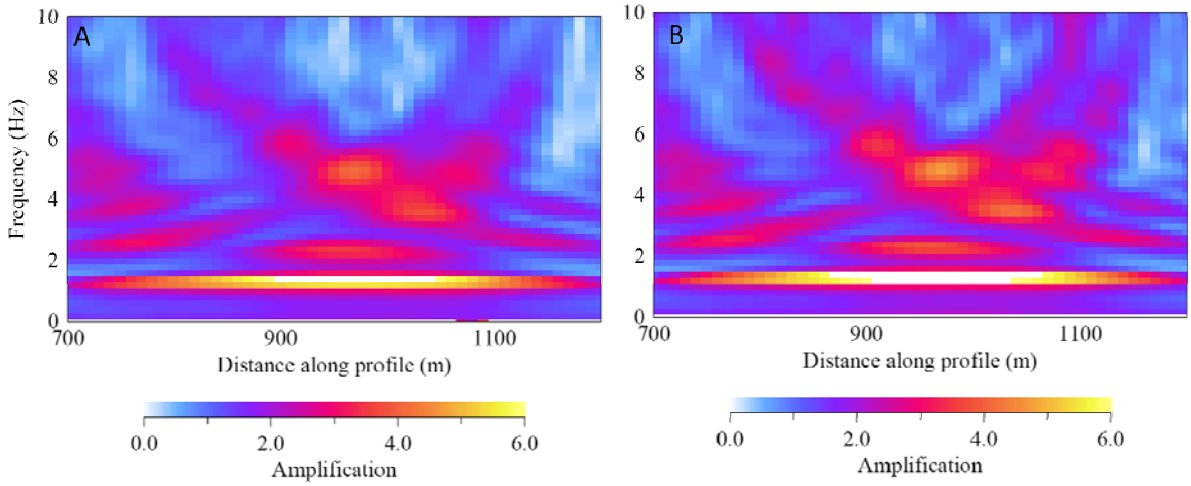

Figure 8. Standard Spectral Ratio for receivers located at the free surface for (A) the layered basin and (B) the gradient-based basin with a visco-elastoelastic soil.

Figure 9 shows the maximum shear strain in the two basins with a visco-elastoplastic soil constitutive model. With the Gabor source, maximum shear strain distribution in the layered basin appears to be not very modified with respect to the viscoelastic case. On the contrary, a kind of layering appears in the gradient-based basin, due to constant nonlinear properties in some depth ranges (we recall that nonlinear properties are homogeneous in layers defined by EPRI (1993) depth ranges, see table 2). At the layers bottom, where nonlinear properties discontinuities are located, the maximum shear strain distribution is modified. With the Northridge source, shear strains are higher and therefore soil nonlinearity is more activated. In this case, shear strain at the bottom of superficial layers in the layered basin is higher than in the viscoelastic case. Moreover, layering of nonlinear properties modifies the shape of maximum shear strain in the gradient-based model like with the Gabor input motion.

Figure 10 shows the logarithm base 10 of the ratio between the maximum shear strain calculated in the layered basin and the gradient-based model with both sources. It clearly shows that shear strain is

higher at the layers bottoms and lower at the layers top in the layered model than in the gradient-based model whatever the input motion. The ratio is higher with the Northridge input motion because the stronger shear modulus decrease and damping increase are more important due to higher strains.

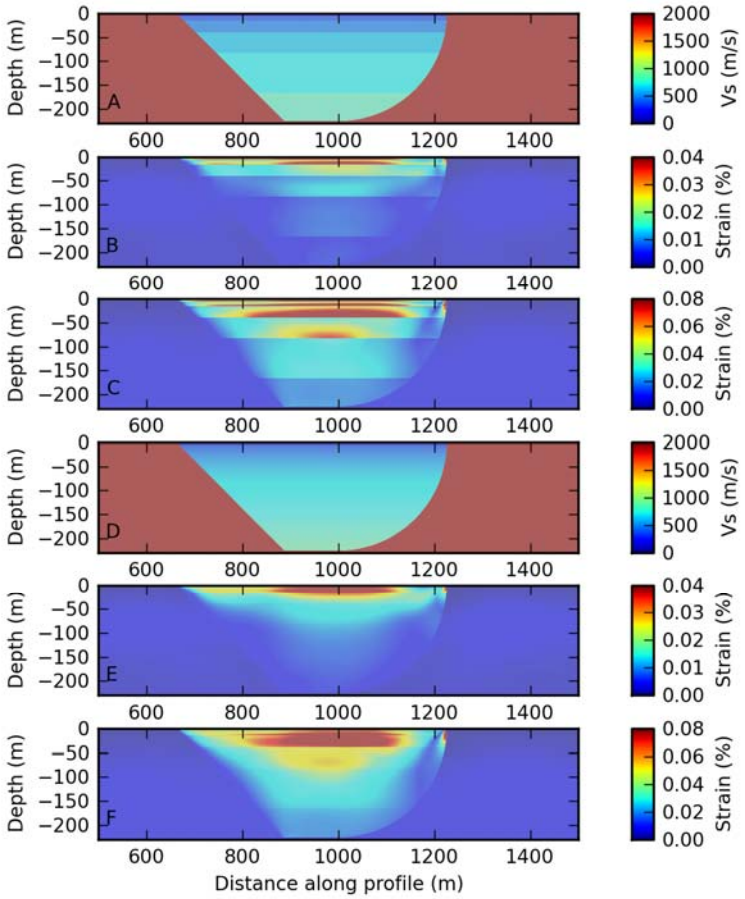

Figure 9. Maximum shear strain calculated in the layered basin (A) and gradient-based basin (D) respectively with the Gabor input motion (B, E) and Northridge input motion (C, F) in a visco-elastoplastic soil.

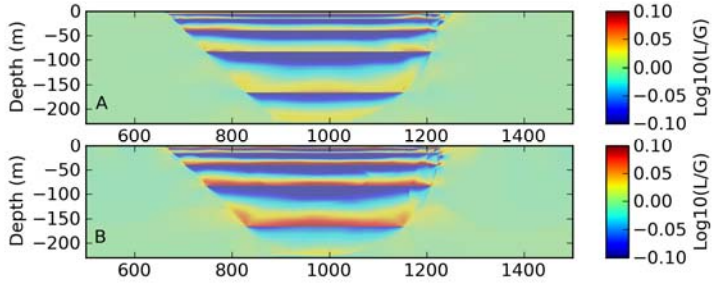

Figure 10. Ratio between the maximum shear strain calculated in the layered basin L and the gradient-based model G with (A) the Gabor input motion and (B) the Northridge one in the visco-elastoplastic soil.

Figure 11 shows the logarithm base 10 of the ratio between the visco-elastoplastic and viscoelastic maximum shear strains in each basin. On the whole, this figure shows that when the soil behavior is nonlinear, shear strain tends to increase at the bottom of superficial layers where shear strain highest values are reached. This increase is stronger for the layered model than for the gradient-based one and particularly stronger for the Northridge input motion than for the Gabor one. This can be explained as follows: the presence of nonlinearity leads to shear modulus decrease, whose amount depends on the soil nonlinear properties and on the input motion (intensity, number of cycles). This decrease leads to the presence of higher impedance contrasts between layers than with a viscoelastic soil. This in turn

leads to stronger wave amplification at the bottom of the layer and therefore to stronger shear strains.
As a matter of fact, this wave amplification has to be compared with wave attenuation related to damping increase in the presence of nonlinearity. When wave damping is stronger than wave amplification, nonlinear soil behavior leads to wave deamplification with respect to the viscoelastic case. This phenomenon appears at the layers top in the basin (layered and gradient-based models) and at depth as well.

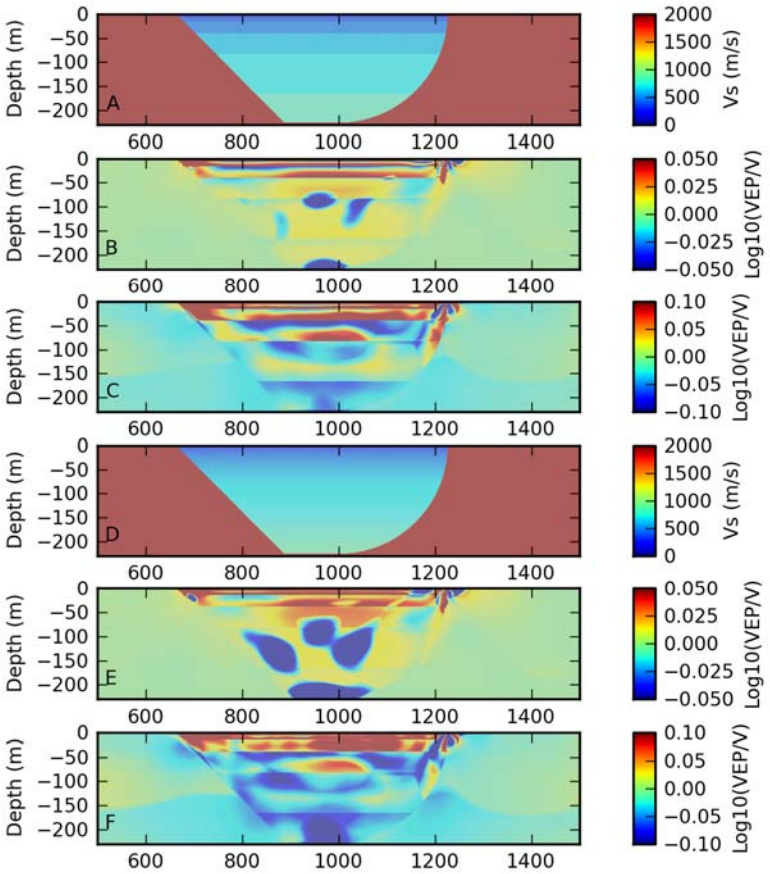

Figure 11. Ratio between the maximum shear strain calculated with the visco-elastoplastic constitutive model (VEP) and the viscoelastic one (V) in the layered basin (A) and gradient-based basin (D) respectively with the Gabor input motion (B, E) and Northridge input motion (C, F).

DISCUSSION AND CONCLUSION

We focused here on the 2D P-SV vertically incident wave propagation in a simple-shaped asymmetric model. We considered two ways of describing the sedimentary infilling properties: the basin was either composed of distinct homogeneous geological layers or was described through properties progressively changing as a function of depth (gradient-based model). In order to study the wave propagation in the two basins with similar soil properties, P and S velocities of the layered basin were deduced from the gradient-based basin ones while density, nonlinear properties remained equal in both models. On the contrary, two different assumptions were made regarding the intrinsic attenuation : it depended on the velocities in the gradient-based model whereas it was kept constant in the layered model. In a next study, we plan to study the wave propagation in the gradient-based model with the same intrinsic attenuation as the layered model. We assessed the influence of sedimentary infilling assumptions on the wave propagation while taking into account linear and nonlinear constitutive models.
SSR computed at the free surface in both basins are very similar because basin properties (geometry and properties) are very close together. However, amplification is stronger at high frequencies in the gradient-based model. This is due to the progressive wave amplification related with velocity decrease

while waves are propagated towards the surface and to a lower velocity at the free surface in the gradient-based basin. We showed too that the shear strain highest values are located in a layered basin at superficial layers bottom where high impedance contrasts lead to wave amplification. At the layers top and near the free surface, maximum shear strain is higher in the gradient-based basin.
The presence of nonlinearity generally enhances wave amplification at the layers bottom due to shear modulus decrease, which increases the impedance contrasts between layers. In a gradient-based model, the shear strain highest values are also controlled by nonlinear properties discontinuities.
This study shows that, when building a geological or geotechnical model to perform a numerical site-specific study, the presence of sharp discontinuities or of soil properties varying smoothly with depth must be carefully assessed. If available, recorded data should be used to understand whether a clear homogeneous or gradient-based model is prevalent. This will help to assess the predominant model of the numerical basin response.

AKCNOWLEDGEMENT
This research was funded by IRSN and the French National research project ANR DEBATE (Risk'nat 2008: ANR-08-RISKNAT-01).

REFERENCES

Assimaki D., Li W. and Kalos A., 2010. A wavelet-based seismogram inversion algorithm for the in-situ characterization of nonlinear soil behaviour. *Pure Appl. Geophys*. DOI 10.1007/s00024-010-0198-6.

Bohlen T. and Saenger E.H., 2006. Accuracy of heterogenous staggered-grid finite-difference modelling of Rayleigh waves. *Geophysics*, **71, 4**, T109-T115.

Bonilla L. F., Archuleta J. R. and Lavallee D., 2005. Hysteretic and dilatant behaviour of cohesionless soils and their effects on nonlinear site response : field data observation and modelling. *Bull. Seism. Soc. Am*., **95, 6**, 2373-2395.

Cerjan, C., D. Kosloff, and M. Reshef, 1985, A nonreflecting boundary condition for discrete acoustic and elastic wave equation: *Geophysics*, **50**, 705-708

Day S.M. and Bradley C.R., 2001. Memory efficient simulation of anelastic wave propagation. *Bull. Seism. Soc. Am*., **91**, 520-531.

Electric Power Research Institute, EPRI, 1993. Guidelines for determining design basis ground motions. *Electric Power Reasearch Institute Technological Report EPRI* TR-102293.

Gélis, C., D. Leparoux, J. Virieux, A. Bitri, S. Operto and G. Grandjean, 2005, Detection of underground cavities: dispersion diagram analysis for synthetic finite difference data, *Journal of Environmental and Engineering Geophysics*: **10**, 111-122

Gélis C. and L.F. Bonilla, 2012. 2D P-SV numerical study of soil-source interaction in a nonlinear basin. Submitted to Geophys. Journal Int

Iai S., Matsunaga Y. and Kameoka T., 1990. Strain space plasticity model for cyclic mobility, *Report of the Port and Harbour Research Institute*, **Vol.29**, pp. 27 –56.

Ishihara K., 1996. Soil Behaviour in Earthquake Geotechnics. Oxford engineering science series 46.Oxford science publications.

Lacave C. and Lemeille F., 2006. Seismic hazard and alpine valley response analysis : generic valley configurations. *Third international Symposium on the effects of surface geology on seismic motion. Grenoble, France, 30 August – 1 September 2006*. Paper number 1.

Liu P.C. and Archuleta J. R., 2006. Efficient modelling of Q for 3D numerical simulation of wave propagation. *Bull. Seism. Soc. Am*. **Vol. 96, No. 4A**, pp. 1352-1358.

Saenger E., Gold N. and Shapiro S., 2000. Modeling the propagation of elastic waves using a modified finite-difference grid. Wave Motion, **Vol. 31**, pp. 77-82.

Towhata I. and K. Ishihara, 1985. Modeling soil behavior under principal axes rotation, *paper presented at the Fifth International Conference on Numerical Methods in Geomechanics, Nagoya, Japan*. Pp 523–530.